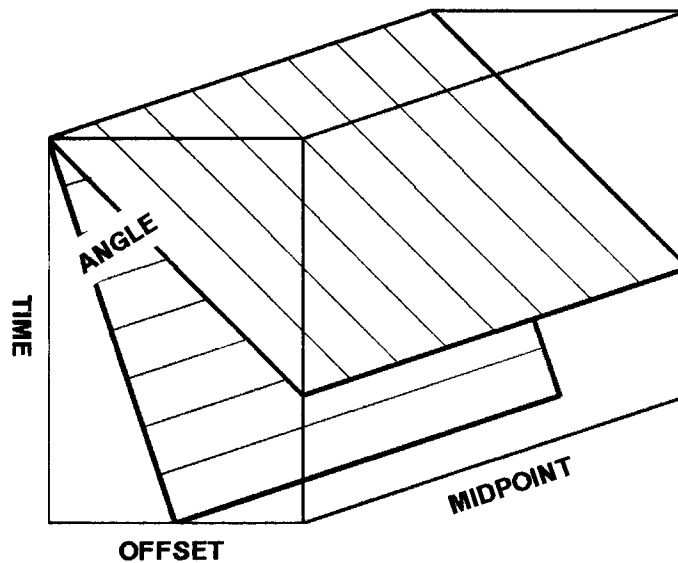


## CHAPTER 3

### Migration of Common Midpoint Radial Traces

#### 3.1. Introduction

The method of radial traces is the most straight forward way of transforming the seismic data into angle-midpoint coordinates. A *radial trace* (introduced by Taner, 1975) is the seismic dataset at a constant ratio of offset to traveltime. It is extracted along a diagonal across a CMP gather. We migrate sections composed of a radial trace taken from each CMP gather at the same angle (Figure 3.1).



**FIGURE 3.1: Common midpoint radial traces.** Shown above is the unstacked data cube. CMP gathers are vertical cross-sections along the shortened side of the cube. Constant offset sections are vertical cross-sections along the elongated direction of the cube. A *radial trace section* is the dataset resampled along a diagonal plane that starts at zero time and zero offset. A *radial trace* is the cross section of this section seen on a CMP gather.

We can write a simple and exact migration equation for seismic data transformed into radial trace sections. This is not true for seismic data organized as constant offset sections, particularly at wide offsets.

### 3.2. Diffractions are Always Hyperbolas

We study the behavior of a point diffraction on radial trace sections for three reasons. First, we can show that the point diffraction is better behaved on radial trace sections than on constant offset sections. Second, because a point scatterer contains all dips, its impulse response is valid for all dips. Third, we can derive a migration equation from the properties of the point diffraction.

Consider the seismic experiment geometry shown in Figure 3.2. The travel time  $t$  for a midpoint  $y$ , half-offset  $h$ , depth  $z$ , and constant velocity  $v$  is given by

$$t = \frac{1}{v} \left[ \sqrt{z^2 + (y - y_0 + h)^2} + \sqrt{z^2 + (y - y_0 - h)^2} \right] \quad (3.1)$$

Travel time is plotted as a function of midpoint and offset according to equation (3.1)

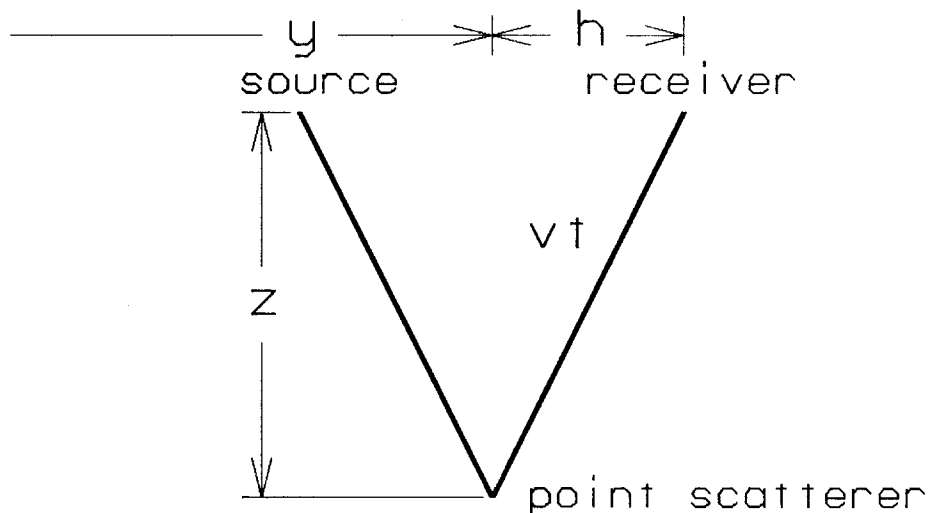


**FIGURE 3.2: Midpoint offset coordinates.** A general seismic recording geometry is a separated source and receiver over a buried reflector.

in Figure 3.3. It resembles a rounded pyramid. The travel time of a source and receiver at various constant offsets are contoured in heavy lines. The zero source - receiver offset contour is a hyperbola. At wide offsets the travel time function has a flattened top and corners. Such a travel time function causes difficulties in designing a stable and accurate migration operator for constant offset sections (Deregowski and Rocca, 1981; Yilmaz and Claerbout, 1980).

Let us determine the point scatterer travel time on a radial trace section. A radial trace section is the seismic data at a constant ratio  $r$  of offset to travel time.

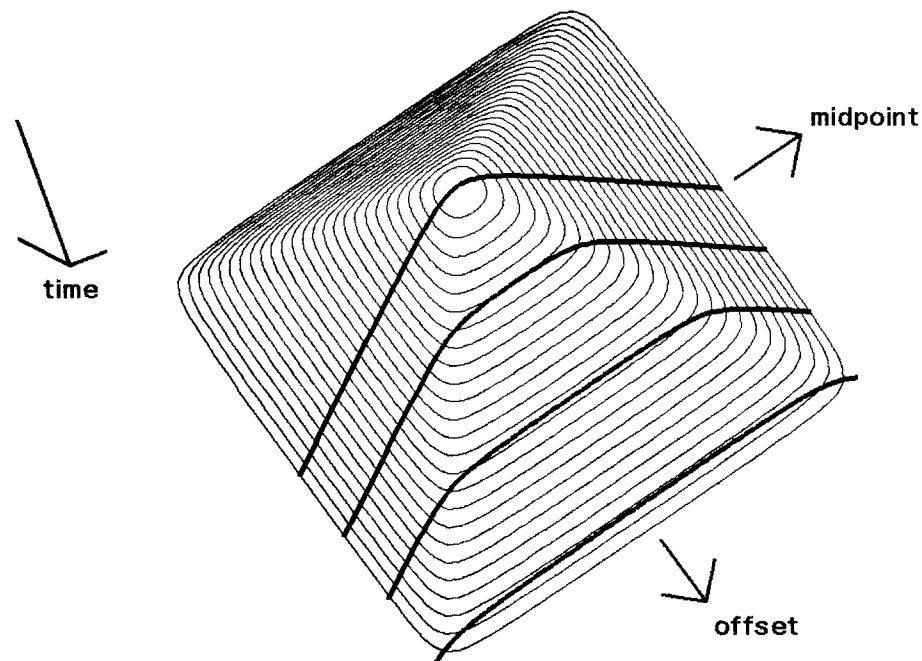


**FIGURE 3.3: Constant offset section travel time pyramid.** Travel time is graphed as a function of midpoint and offset according to equation (3.1). A point scatterer is at the apex of the "pyramid". Travel time is contoured for fixed travel time (rings) and fixed source-receiver offset (heavy lines). Only the zero offset contour is a perfect hyperbola. The other fixed offset curves are flattened at the top and present problems to migration operators. The scaling parameters are  $z=100$ ,  $\max h$  and  $y$  are 800,  $\Delta h=250$ , and  $\nu=1$ .

$$\boxed{r = \frac{h}{t}} \quad (3.2)$$

Substituted into equation (3.1), the travel time function becomes

$$t = \frac{2}{v} \left( \frac{z^2}{1 - \frac{4r^2}{v^2}} + y^2 \right)^{1/2} \quad (3.3)$$

Equation (3.3) is that of a hyperbola with the z axis scaled by

$$z' = z \left( 1 - \frac{4r^2}{v^2} \right)^{-1/2} \quad (3.4)$$

Equation (3.3) is contoured for various values of  $r$  on the travel time pyramid in Figure 3.4. The contours are always hyperbolas. It is easy to design a migration operator for such a travel time function.

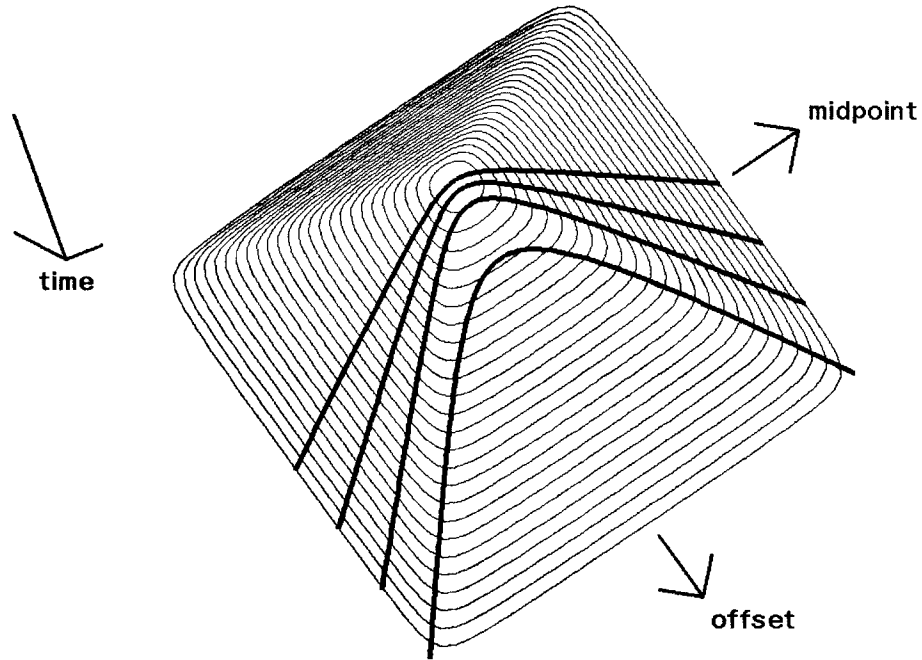


**FIGURE 3.4: Radial trace travel time pyramid.** Equation (3.1) is contoured for fixed travel time in the same manner as the previous figure. Contours of fixed radial parameter  $r$  are superimposed on the travel time pyramid. Such contours are always hyperbolas and easy to design migration operators for. The increment for  $r$  is 300.

### 3.3. Migration Equation for Common Midpoint Radial Traces

The equation for collapsing the hyperbolas seen on a zero offset section was derived in appendix E.

$$\frac{\partial P}{\partial z} = -2i \frac{\omega}{v} \sqrt{1 - \gamma^2} P \quad (\text{E.20})$$

This is the equation used to migrate conventionally stacked sections. We rescale  $z$  in equation (E.20) according to equation (3.4) to obtain an equation for migrating radial traces.

$$\boxed{\frac{\partial P}{\partial z} = -2i \frac{\omega}{v} \left( \frac{1 - \gamma^2}{1 - \frac{4r^2}{v^2}} \right)^{1/2} P} \quad (\text{3.5})$$

### 3.4. Partial Migration

The derivation of the migration equation assumed constant velocity. Chapter 4 shows how to extend this theory to a stratified earth. The migration equation (3.5) is used for converting a radial trace section into an earth image all in one step. If we introduce a *partial migration* based on radial trace sections, the velocity term all but drops out of the migration equation.

Conventional processing migrates unstacked data in two steps. First is an offset-only operation: CMP stacking. Second is a midpoint-only operation: migration of CMP stacks. Appendix E shows these operations assume zero dip and zero offset, approximations that become increasingly inaccurate as the dip of a reflector steepens. Yilmaz and Claerbout (1980) derived a compensatory migration operation to be applied to constant offset sections before CMP stacking. However, their operator was had stability problems because of a pole. A radial trace reformulation avoids this problem.

### 3.5. Partial Migration Equation for Midpoint Radial Traces

The partial migration equation is derived by subtracting the operators that represent conventional processing from the full migration operator (3.5) to find a residual migration operator. The gist of the migration operator is the square root.

$$\left( \frac{1 - Y^2}{1 - \frac{4r^2}{v^2}} \right)^{1/2} \quad (3.6)$$

This square root is a *phase shift* in the depth direction and embodies the geometry of processing coordinate system.

The most basic function of the migration operator is to convert time to depth. This is independent of dip ( $Y=0$ ) and offset ( $r=0$ ). The phase shift of equation (3.6) then becomes unity. The migration-like part of the phase shift that operates on midpoint sections only is found by setting  $r$  equal to zero and subtracting the time to depth conversion.

$$\left( 1 - Y^2 \right)^{1/2} - 1 \quad (3.7)$$

Likewise, the moveout-like part of the phase shift that operates on offset only is found by setting  $Y$  equal to zero and subtracting the time to depth conversion.

$$\left( 1 - \frac{4r^2}{v^2} \right)^{-1/2} - 1 \quad (3.8)$$

The partial migration operator is found by subtracting equations (3.7) and (3.8) from (3.6). Square roots are expanded to the first order.

$$\begin{aligned} \left( \frac{1 - Y^2}{1 - \frac{4r^2}{v^2}} \right)^{1/2} - \left[ \left( 1 - Y^2 \right)^{1/2} - 1 \right] - \left[ \left( 1 - \frac{4r^2}{v^2} \right)^{-1/2} - 1 \right] \\ \approx \left( 1 - \frac{2r^2 Y^2}{v^2} \right)^{1/2} \end{aligned} \quad (3.9)$$

The partial migration equation containing the phase shift of equation (3.9) is actually velocity independent. We insert the phase shift of equation (3.9) into a migration

equation (3.5). Then we convert depth to migrated time using  $dz = 2vd\tau$  and rewrite  $Y = vk_h / 2\omega$ .

$$\frac{\partial P}{\partial \tau} = -i\omega \left( 1 - \frac{\tau^2 k_y^2}{2\omega^2} \right)^{1/2} P \quad (3.10)$$

Equation (3.10) is used for partial migration of radial trace sections.

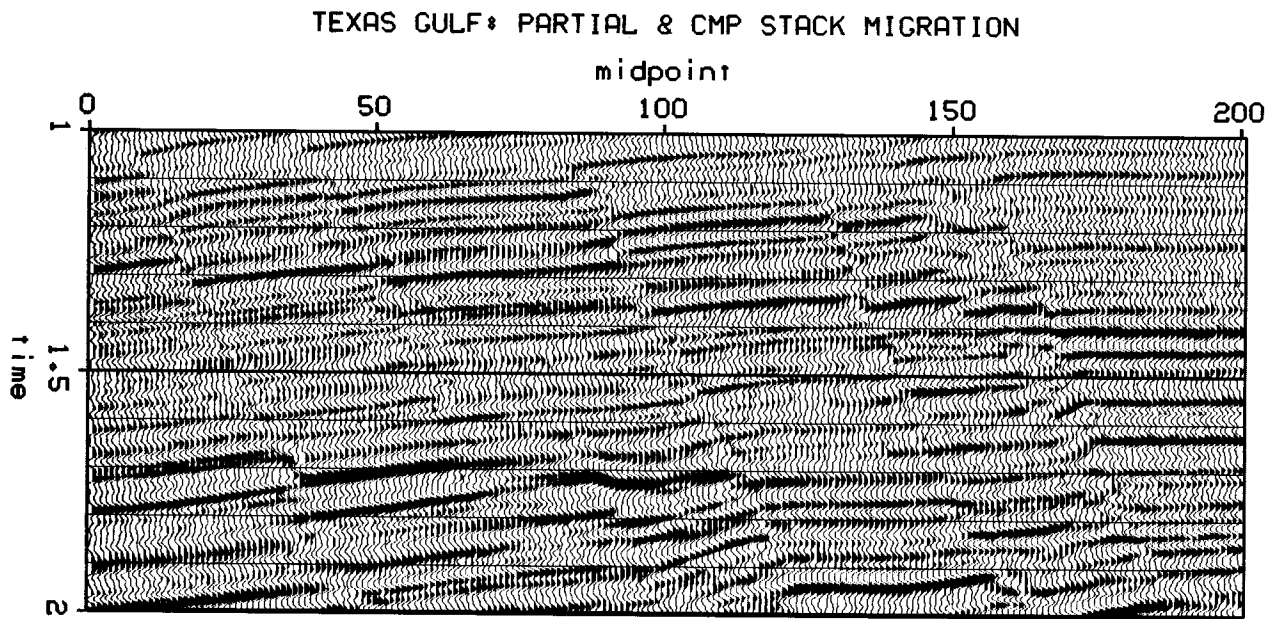
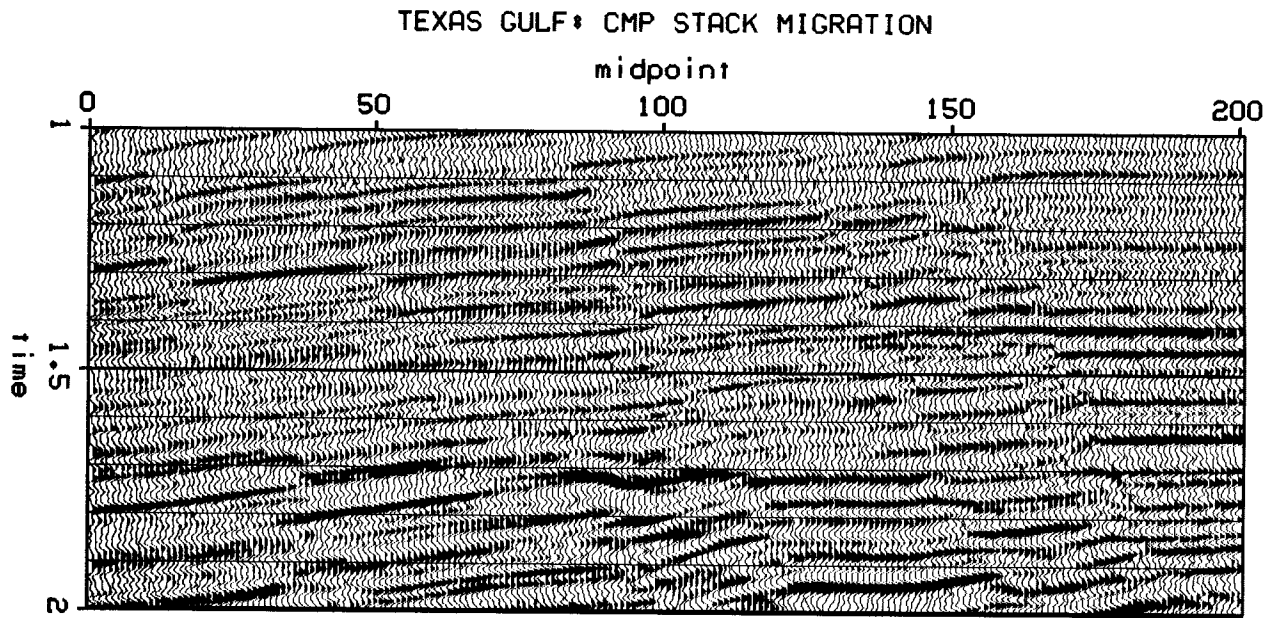
### 3.6. Partial Migration Processing Sequence

A radial trace partial migration sequence is:

- (1) First, construct radial trace sections by assembling the radial trace for a given  $\tau$  from each CMP gather (Figure 3.1). At least two dozen radial parameters  $\tau$  should be used in order to convert back to CMP gathers after the partial migrations. The range of  $\tau$  should span the data present on a CMP gather.
- (2) Second, migrate each radial trace section using some solution to equation (3.10). Note that equation (3.10) is identical to the conventional stack migration equation (E.20), except velocity  $v$  has been replaced by radial parameter  $\tau / 1.414$ . A quick conventional migration program can be used to migrate these radial trace sections.
- (3) Third, invert the migrated results for CMP gathers.
- (4) Finally, perform conventional processing including CMP gather velocity analysis, CMP stacking, and migration of CMP stacks.

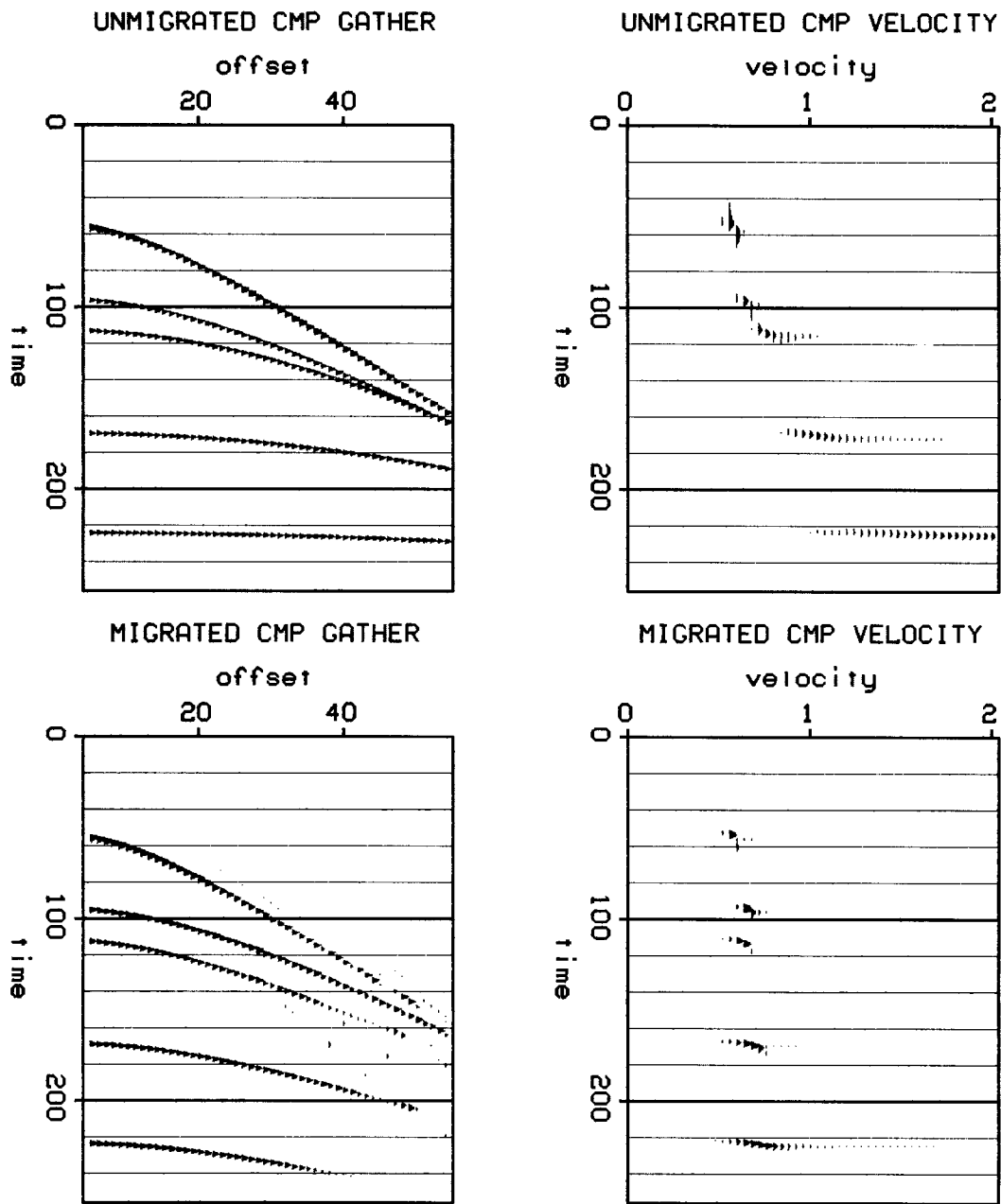
### 3.7. Partial Migration Results

Figure 3.5 shows how radial trace partial migration has improved the imaging of steep reflectors on a growth fault dataset over conventional processing. The improvement is not as great as for slant stack processing (Figure 2.3). Figure 3.6 shows how radial trace partial migration has improved velocity analysis on a synthetic



**FIGURE 3.5: Radial trace partial migration vs. conventional migration.** On the top is a CMP stack migration of a Texas Gulf coast dataset. Below is the same process after radial trace partial migration, that improves the images of the steep dipping fault plane reflections.





**FIGURE 3.6: Velocity analysis after radial trace partial migration.** In the upper left is a CMP gather taken from the synthetic dataset of Figure 2.9 before partial migration (midpoint 50). In the upper right is a velocity analysis of this gather. The steeper the reflector dip, the greater the velocity falsification and defocusing. On the bottom are the CMP gather and velocity analysis after partial migration. The curvature of dipping events on the CMP gather resembles that of flat events. This explains why both the velocity analysis and migrated images are more accurate and look sharper.

model (Figure 2.9) with steeply dipping reflectors. The false high velocity values and smearing due to dip have been eliminated by this method.

### 3.8. Comparison with Other Partial Migration Methods

Several recently developed partial migration algorithms are closely related to the results presented in this paper. They are all essentially velocity independent, but differ in whether they use constant offset sections or radial traces and in the form of the migration equation. They are summarized in the following table:

<b>Partial Migration Comparisons</b>			
technique		accuracy	workability
Yilmaz and Claerbout; (Bolondi, et. al.)	$P_{t\tau} = \alpha \left( \frac{h}{t} \right)^\beta P_{zz}$	"15°" offset angles	vertical grid resampling, only one offset needed
Hale	$\omega \left[ 1 - \frac{h^2 k_x^2}{t^2 \omega^2} \right]^{1/2}$	wide offset angles	recompute phase shift, only one offset needed
Ottolini, this thesis	$\omega \left[ 1 - \frac{r^2 k_x^2}{2\omega^2} \right]^{1/2}$	>15° offset angles	interpolate many offsets, easy migration

The main difference between these three schemes is whether they implement the key parameter  $r = h/t$  on constant offset sections or radial trace sections. Offset angle accuracies are similar, but their workabilities differ. The first two methods are nice because they work on a single constant offset section, while radial traces require a gather of offsets. However, the constant offset equations are beset with numerical difficulties.

### **3.9. Conclusions**

- (1) Radial trace coordinates have certain theoretical and practical advantages over CMP stacks and constant offset sections.
- (2) An effective and economical velocity insensitive partial migration scheme can be implemented in radial trace coordinates.
- (3) In some practical sense, radial trace partial migration is better than other constant offset schemes and in some ways worse. At this time, I call it a stand-off.